Quantum engineering of heterostructure detectors for enhanced performance

Michael Stroscio
UNIVERSITY OF ILLINOIS

05/23/2017
Final Report

REPORT DOCUMENTATION PAGE

Form Approved
OMB No. 0704-0188

The public reporting burden for this collection of information is estimated to average 1 hour per response, including the time for reviewing instructions, searching existing data sources, gathering and maintaining the data needed, and completing and reviewing the collection of information. Send comments regarding this burden estimate or any other aspect of this collection of information, including suggestions for reducing the burden, to the Department of Defense, Executive Service Directorate (0704-0188). Respondents should be aware that notwithstanding any other provision of law, no person shall be subject to any penalty for failing to comply with a collection of information if it does not display a currently valid OMB control number.

PLEASE DO NOT RETURN YOUR FORM TO THE ABOVE ORGANIZATION.

1. REPORT DATE *(DD-MM-YYYY)*	2. REPORT TYPE	3. DATES COVERED *(From - To)*
26-05-2017	FINAL	30-09-15 to 29-03-17

4. TITLE AND SUBTITLE

Quantum Engineering of States in Heterostructure-based Detectors for Enhance Performance

5a. CONTRACT NUMBER

5b. GRANT NUMBER

FA9550-15-1-0493

5c. PROGRAM ELEMENT NUMBER

6. AUTHOR(S)

Michael A. Stroscio

5d. PROJECT NUMBER

5e. TASK NUMBER

5f. WORK UNIT NUMBER

7. PERFORMING ORGANIZATION NAME(S) AND ADDRESS(ES)

College of Engineering
University of Illinois at Chicago
851 S. Morgan St., MS-154
Chicago, IL 60607

8. PERFORMING ORGANIZATION REPORT NUMBER

9. SPONSORING/MONITORING AGENCY NAME(S) AND ADDRESS(ES)

Air Force Office of Scientific Research
875 N. Randolph, Ste.325.
Arlington Virginia, 22203

10. SPONSOR/MONITOR'S ACRONYM(S)

AFOSR

11. SPONSOR/MONITOR'S REPORT NUMBER(S)

12. DISTRIBUTION/AVAILABILITY STATEMENT

DISTRIBUTION A: Approved for Public Release

13. SUPPLEMENTARY NOTES

14. ABSTRACT

The investigators have undertaken several quantum engineering and phonon engineering efforts underlying the enhancement of the performance of nanostructure-based sensors and electronicoptoelectronic devices. These include: design of novel photodetectors relying on phonon-assisted transitions as well as photon absorption events; AlGaAs/GaAs triple well photodetector; spontaneous polarization induced electric fields in nanostructures. This research includes modeling and theory of quantum confined structures as well as related experimental studies.

15. SUBJECT TERMS

Heterostructure devices; phonon-assisted transitions; quantum-well devices

16. SECURITY CLASSIFICATION OF:			17. LIMITATION OF ABSTRACT	18. NUMBER OF PAGES	19a. NAME OF RESPONSIBLE PERSON
a. REPORT	b. ABSTRACT	c. THIS PAGE			Michael A. Stroscio
U	U	U	None	19	**19b. TELEPHONE NUMBER** *(Include area code)* (847) 962-4955

Reset

Standard Form 298 (Rev. 8/98)
Prescribed by ANSI Std. Z39.18
Adobe Professional 7.0

INSTRUCTIONS FOR COMPLETING SF 298

1. REPORT DATE. Full publication date, including day, month, if available. Must cite at least the year and be Year 2000 compliant, e.g. 30-06-1998; xx-06-1998; xx-xx-1998.

2. REPORT TYPE. State the type of report, such as final, technical, interim, memorandum, master's thesis, progress, quarterly, research, special, group study, etc.

3. DATES COVERED. Indicate the time during which the work was performed and the report was written, e.g., Jun 1997 - Jun 1998; 1-10 Jun 1996; May - Nov 1998; Nov 1998.

4. TITLE. Enter title and subtitle with volume number and part number, if applicable. On classified documents, enter the title classification in parentheses.

5a. CONTRACT NUMBER. Enter all contract numbers as they appear in the report, e.g. F33615-86-C-5169.

5b. GRANT NUMBER. Enter all grant numbers as they appear in the report, e.g. AFOSR-82-1234.

5c. PROGRAM ELEMENT NUMBER. Enter all program element numbers as they appear in the report, e.g. 61101A.

5d. PROJECT NUMBER. Enter all project numbers as they appear in the report, e.g. 1F665702D1257; ILIR.

5e. TASK NUMBER. Enter all task numbers as they appear in the report, e.g. 05; RF0330201; T4112.

5f. WORK UNIT NUMBER. Enter all work unit numbers as they appear in the report, e.g. 001; AFAPL30480105.

6. AUTHOR(S). Enter name(s) of person(s) responsible for writing the report, performing the research, or credited with the content of the report. The form of entry is the last name, first name, middle initial, and additional qualifiers separated by commas, e.g. Smith, Richard, J, Jr.

7. PERFORMING ORGANIZATION NAME(S) AND ADDRESS(ES). Self-explanatory.

8. PERFORMING ORGANIZATION REPORT NUMBER. Enter all unique alphanumeric report numbers assigned by the performing organization, e.g. BRL-1234; AFWL-TR-85-4017-Vol-21-PT-2.

9. SPONSORING/MONITORING AGENCY NAME(S) AND ADDRESS(ES). Enter the name and address of the organization(s) financially responsible for and monitoring the work.

10. SPONSOR/MONITOR'S ACRONYM(S). Enter, if available, e.g. BRL, ARDEC, NADC.

11. SPONSOR/MONITOR'S REPORT NUMBER(S). Enter report number as assigned by the sponsoring/ monitoring agency, if available, e.g. BRL-TR-829; -215.

12. DISTRIBUTION/AVAILABILITY STATEMENT. Use agency-mandated availability statements to indicate the public availability or distribution limitations of the report. If additional limitations/ restrictions or special markings are indicated, follow agency authorization procedures, e.g. RD/FRD, PROPIN, ITAR, etc. Include copyright information.

13. SUPPLEMENTARY NOTES. Enter information not included elsewhere such as: prepared in cooperation with; translation of; report supersedes; old edition number, etc.

14. ABSTRACT. A brief (approximately 200 words) factual summary of the most significant information.

15. SUBJECT TERMS. Key words or phrases identifying major concepts in the report.

16. SECURITY CLASSIFICATION. Enter security classification in accordance with security classification regulations, e.g. U, C, S, etc. If this form contains classified information, stamp classification level on the top and bottom of this page.

17. LIMITATION OF ABSTRACT. This block must be completed to assign a distribution limitation to the abstract. Enter UU (Unclassified Unlimited) or SAR (Same as Report). An entry in this block is necessary if the abstract is to be limited.

ANNUAL TECHNICAL (Oct15-Mar17) REPORT ON

AFOSR FA9550-15-1-0493

"Quantum Engineering of States in Heterostructure-based Detectors for Enhance
Performance --- Revision"

(1) Introduction

This research effort has the goals of exploiting and integrating forefront developments in nanoscience and nanoelectronics to conceive, design, fabricate, and test flexible sensors with greatly enhanced performance. To accomplish these goals, this effort focused on the design of novel heterostructure-based sensors that integrate multiple-quantum-well elements to yield enhanced performance based on quantum engineering of both electronic and phononic states. Specifically, in this work the unwanted thermally excited carrier contribution in these heterostructure-based photodetectors has been reduced by using phonon-assisted transitions to design structures having deeper initial quantum states. This novel design has been modeled and characterized experimentally for a prototypical heterostructure. In addition, this effort addressed the optimization of these photodetectors through tailoring carrier interactions in these reduced dimensional structures.

(2) List of Appendixes --- N/A

(3) Statement of Problem Studied

This research program addressed systematic theoretical and experimental investigations of nanostructure-based electronic and optoelectronic structures with the goal of facilitating major improvements in the performance levels of nanodevices beyond the current state-of-the-art. In particular, this program focuses on research thrusts with objectives including: model, design, fabricate, and experimentally characterize nano-device structures for enhanced charge transport & collection; model, design, fabricate, and experimentally characterize such nanodevices to optimize device structures with quantum-engineering and phonon-assisted transitions in nanostructures. Quantum engineering of nano-structures is emphasized. Related quantum-based structures – including those with spontaneous polarizations are included.

(4) Summary of Most Important Results

The most important results obtained during this period of this effort include: electrical and optical studies of components of devices and systems of quantum-dot-based optoelectronic devices; electronic and optical properties of quantum dots in ensembles; characterization of quantum-dot blinking phenomena; characterization of phonon modes in quantum dots; and extending a theory band formation in an array of colloidal quantum dots embedded in conductive polymer. Specific results were obtained on the following topics:

This research has focused on exploring the design and experimental verification of a concept for novel photodetectors with dramatic enhancement in detectivity, based on rapid interface phonon-assisted transitions combined with quantum engineering of phonon and electron states in nanostructures. Based on the concepts we introduced previously (Stroscio (1996), Kisin et al. (1997), Stroscio et al. 1999, and Stroscio and Dutta (2001) for heterosturcture lasers, which have resulted in extremely large enhancements in the optical gain of quantum-well-based lasers, this work examines dramatic enhancement of photodetectivity in novel quantum-well based photodetectors in the first known embodiment that facilitates the detection of photons over a wide range of frequencies. In preliminary studies (Lan et al. (2014)), we have identified several different heterostructures for these photodetectors – with specific materials, compositions -- suitable as photodetectors incorporating phonon-assisted transitions: one based on GaAlAs/GaAs material system, one based on InGaAs/InAs material system and the other one base on InAlAs/InP material system. These designs bear similarities to phonon-assisted quantum cascade lasers discussed in papers (Spagnolo et al. (2002), Williams et al. (1999), Menon et al. (2002)) that make reference to our earlier treatments of phonons in heterostructures (Stroscio (1996), Kisin et al. (1997), and Stroscio et al. 1999).

In addition to interface phonon engineering, a novel feature of the designs considered herein is a double-well region that allows tuning of energy state defferences so that a double resonance condition (Stroscio et al. (1999)) - for a pair of degenerate states and a pair of states separated by an interface phonon energy – can be satisfied. To our knowledge, this novel double-well system has not been used in conjunction with phonon-assisted transitions in the past; however, the double-well component is critical to the tunability of the low noise photodetectors advocated in this proposal. Herein, we consider a triple quantum-well structure with one single well and one double well; the relationship between the energy levels should be, as in Fig. 1.
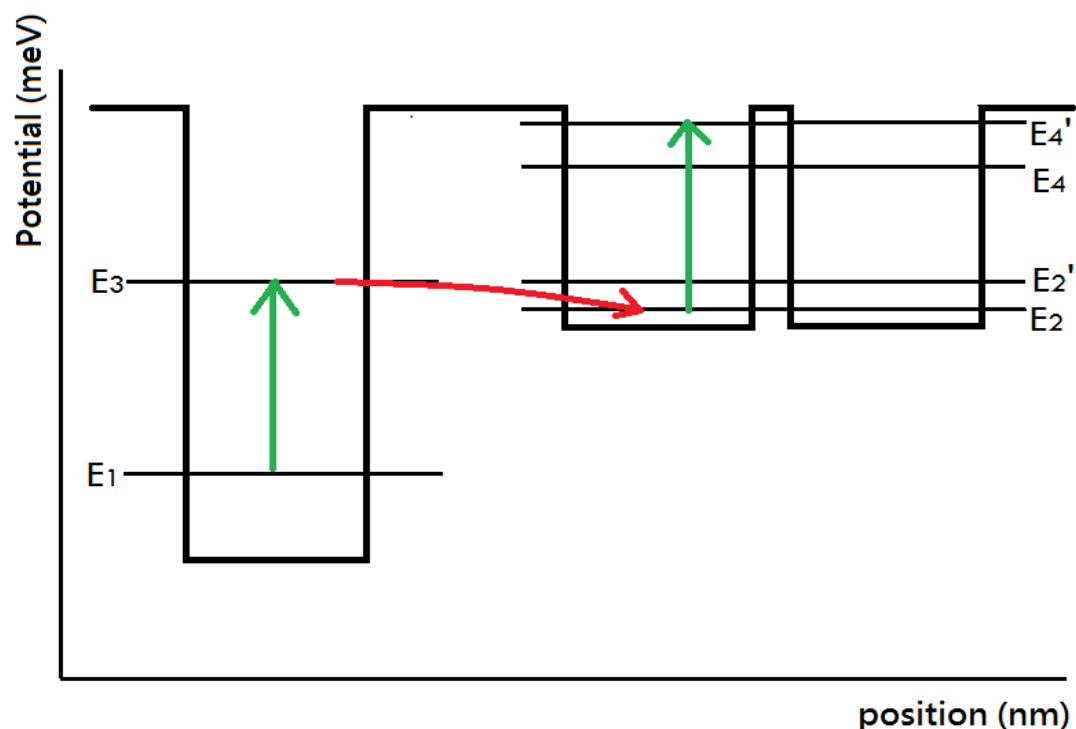
Figure 1. Structure of single-well—double well ehterostructure-based photodetector with intermediate states E_3 and E_2 that provide a channel for rapid phonon-assisted transitions of an electron from state E_3 to state E_2 as a result of the emission of an interface phonon.

From the energy level states in Figure 1, it follows that:

$E_3 = E_{2'}$

$E_3 - E_1 = E_{4'} - E_2 = E_{photon}$

And

$E_{2'} - E_2 = E_{phonon}$

The energy-level structure depicted in Figure 1 for the novel photodetector facilitates the absorption of a photon, emission of a phonon, and the absorption of a photon with the same wavelength as the original photon. E_1 is the first energy level of the single well, and E_3 is the second energy level. In addition, E_2, $E_{2'}$, E_4, and $E_{4'}$ represent the first, second, third, and forth energy levels for the double quantum well. With reference to the Figure 1, it is clear that there will be a dramatic signal-to-noise enhancement in the current, $I_{sn,E1}$, from the deepest state E_1, relative to $I_{sn,E2}$, from the deepest state E_2 (without phonon-assisted transition and second photon absorption), as given by the Richardson formula:

3

$$\frac{I_{sn,E_1}}{I_{sn,E_2}} = \frac{e^{-\frac{2E_{photon}-E_{phonon}}{kT}}}{e^{-\frac{E_{photon}}{kT}}} = e^{-\frac{E_{photon}-E_{phonon}}{kT}}$$

In this equation, $E_3 - E_1 = E_{4'} - E_2 = E_{photon}$ and $E_{2'} - E_2 = E_{phonon}$.
For example if,

$$\frac{E_{photon}-E_{phonon}}{kT} = 8$$

a dramatic 1/3,000 reduction in the noise is predicted. It is this reduction in noise through the quantum engineering of electronic and phononic states that is pursued in this research.

Based on the previous description, it is clear that this photodetector design exploits the use of rapid interface-phonon assisted electron transitions between the single quantum well (left) and and the double quantum well (right). In operation the photodetector works as follows: (1) a single photon is absorbed in the left single well; (2) the excited electron emits an interface phonon and, consequently, makes a transition to the double well on the right; (3) the electron then absorbs a photon and reaches the ionization limit where it is detected. The key innovations in this design are the tunable double-well structure coupled with the use of interface-phonon-assisted transitions so that the initial state of the electron is approximately twice as deep as in the case of a single-quantum well photodetector. This extra depth leads to a dramatic reduction in the unwanted thermal excitation from the initial state as estimated on the bottom right.

In this program a number of different heterostructure systems have been designed that facilitate phonon-assisted transitions in a single-well—double-well heterostructure with two pairs of energy levels having equal separations between eigenenergies for two-photon absorption.

After many calculations are made, one set of single-double well design parameter for GaAlAs material that optimizes the signal-to-noise in the photodetector is found as shown in Figure 2.
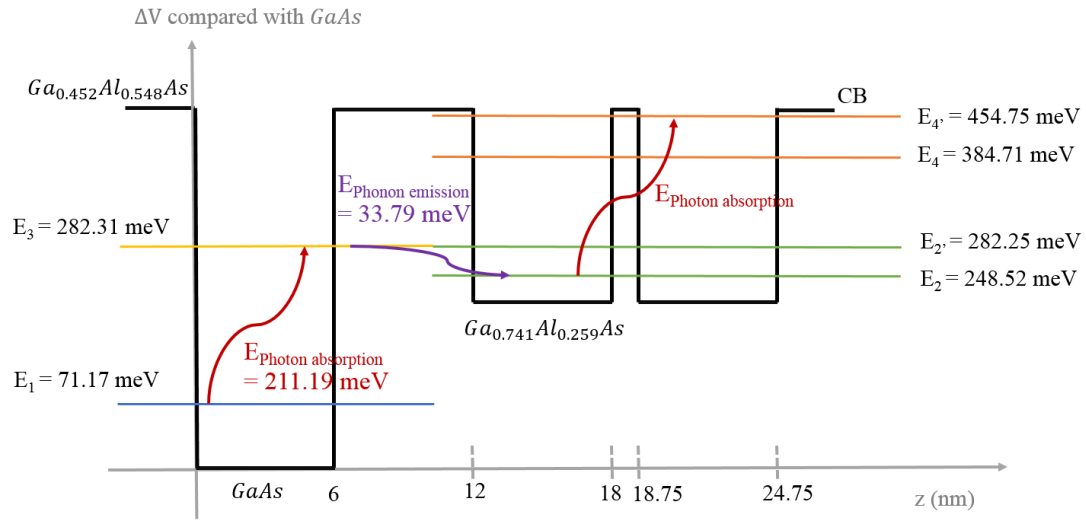
4

Figure 2. **Result of signal-to-noise enhanced photodetector in $Ga_{1-x}Al_xAs$ material.**

For the single well, $Ga_{0.452}Al_{0.548}As$ is used as the barrier, and GaAs as the well. The potential of the single well then turns out to be 457.849 meV. For the double well, $Ga_{0.452}Al_{0.548}As$ is still the barrier, both outside the double well and between it, and now we use $Ga_{0.741}Al_{0.259}As$ as the well. A depth of 241.457 meV as potential of the double well is obtained.

In this result, we have the width of single well as 6 nm, and the width of each wells in double well as 6 nm as well. The barrier between the double well is 0.75 nm, and the barrier between single well and double well is 6 nm.

The energy states in single well then turns out to be $E_1 = 71.17$ meV, and $E_3 = 282.31$ meV. In the double well, energy states are $E_2 = 248.52$ meV, $E_{2'} = 282.52$ meV, $E_4 = 384.71$ meV, and $E_{4'} = 454.75$ meV as shown in Figure 2.

The whole process of this signal-to-noise photodetector in this design works as follows:

i.   From the E_1 state, an electron absorbs one photon energy which equals to 211.19 meV, having wavelength of 5871.49 nm, and jumps to E_3 state.

ii. The electron emits one phonon energy of 33.79 meV, and falls down to the state E_2.

iii. Absorbing another photon with 206.23 meV (wavelength = 6012.70 nm) which having similar energy as the first one, the electron jumps to $E_{4'}$, which is very close to the barrier level of $Ga_{0.452}Al_{0.548}As$, and will be detected.

5

A range of light source which includes 5871.49 nm and 6012.70 nm will be detected by this detector.

For $In_{1-y}Ga_yAs$, the need parameters must be specified; the parameters includes the discontinuity of conduction band energy for $In_{1-y}Ga_yAs$ that having different concentration of y, and its electron effective mass.

The total band gap energy discontinuity for $In_{1-x-y}Al_xGa_yAs/AlAs$ is:

$$\Delta V = [2.093x + 0.629y + 0.577x^2 + 0.436y^2 + 1.013xy - 2.0x^2(1 - x - y)] \, eV$$

and the band alignment is 47% of the total discontinuity in valence band, which means:

$$\Delta V_{VB} = 0.47$$

$$\Delta V_{CB} = 0.53$$

The electron effective mass for $In_{1-x-y}Al_xGa_yAs/AlAs$ is:

$$m^* = (0.0427 + 0.0685x)m_0$$

where $m_0 = 9.10938215 \times 10^{-31}$.

Therefore, if x = 0 is assumed in all the parameters, we can get parameters in $In_{1-y}Ga_yAs/AlAs$ follows:

$$\Delta V' = (0.629y + 0.436y^2) \, eV$$

and since $\Delta V_{VB} = 0.47$ and $\Delta V_{CB} = 0.53$, the conduction band discontinuity of $In_{1-y}Ga_yAs/AlAs$ is:

$$\Delta V" = [(0.629y + 0.436y^2) \times 0.53] \, eV$$

Also,

$$m^{*\prime} = 0.0427m_0$$

where $m_0 = 9.10938215 \times 10^{-31}$.

Since Figure 3 illustrates the association of parameters of the $In_{1-y}Ga_yAs$ single-double well design and with different regions of the structure.
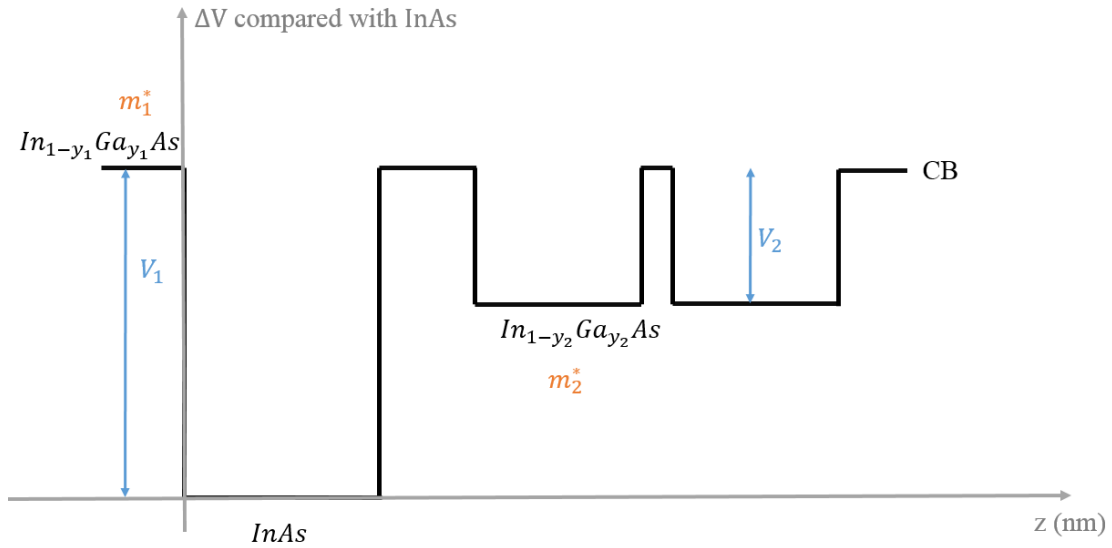
Figure 3. **Single-double quantum well design in In$_{1-y}$Ga$_y$As material.**

For the voltage level changing compared with InAs of wells and barriers in Figure 3, we have,

$$V_1 = \left(0.629y_1 + 0.436y_1^2\right) \times 0.53$$

$$V_1 - V_2 = \left(0.629y_2 + 0.436y_2^2\right) \times 0.53$$

and the corresponding electron effective mass are,

$$m_1^* = 0.0427m_0$$

$$m_2^* = 0.0427m_0$$

with $m_{InAs}^* = 0.067m_0$.

The wave equations for the In$_{1-y}$Ga$_y$As single-double quantum well structure can now be described as follows:

$$-\frac{\hbar^2}{2 \times 0.0427m_0}\frac{\partial^2}{\partial z^2}\varphi_1(z) + \left[\left(0.629y_1 + 0.436y_1^2\right) \times 0.53\right]\varphi_1(z) = E\varphi_1(z)$$

when z ≤ 0

$$-\frac{\hbar^2}{2 \times 0.0427m_0}\frac{\partial^2}{\partial z^2}\varphi_2(z) = E\varphi_2(z)$$

when $0 \leq z \leq z_1$

$$-\frac{\hbar^2}{2 \times 0.0427m_0}\frac{\partial^2}{\partial z^2}\varphi_3(z) + \left[\left(0.629y_1 + 0.436y_1^2\right) \times 0.53\right]\varphi_3(z) = E\varphi_3(z)$$

when $z_1 \leq z \leq z_2$

$$-\frac{\hbar^2}{2 \times 0.0427m_0}\frac{\partial^2}{\partial z^2}\varphi_4(z) + \left[\left(0.629y_2 + 0.436y_2^2\right) \times 0.53\right]\varphi_4(z) = E\varphi_4(z)$$

when $z_2 \leq z \leq z_3$

$$-\frac{\hbar^2}{2 \times 0.0427m_0}\frac{\partial^2}{\partial z^2}\varphi_5(z) + \left[\left(0.629y_1 + 0.436y_1^2\right) \times 0.53\right]\varphi_5(z) = E\varphi_5(z)$$

when $z_3 \leq z \leq z_4$

$$-\frac{\hbar^2}{2 \times 0.0427m_0}\frac{\partial^2}{\partial z^2}\varphi_6(z) + \left[\left(0.629y_2 + 0.436y_2^2\right) \times 0.53\right]\varphi_6(z) = E\varphi_6(z)$$

when $z_4 \leq z \leq z_5$

$$-\frac{\hbar^2}{2 \times 0.0427m_0}\frac{\partial^2}{\partial z^2}\varphi_7(z) + \left[\left(0.629y_1 + 0.436y_1^2\right) \times 0.53\right]\varphi_7(z) = E\varphi_7(z)$$

when $z_5 \leq z$

where $\hbar = 1.054571628 \times 10^{-34}$, and $m_0 = 9.10938215 \times 10^{-31}$.

Figure 4 illustrates the demands for signal-to-noise enhanced photodetector.

In $In_{1-y}Ga_yAs$ design, the larger the y is, which means when the concentration of GaAs is higher, the higher the conduction band level will be.

8

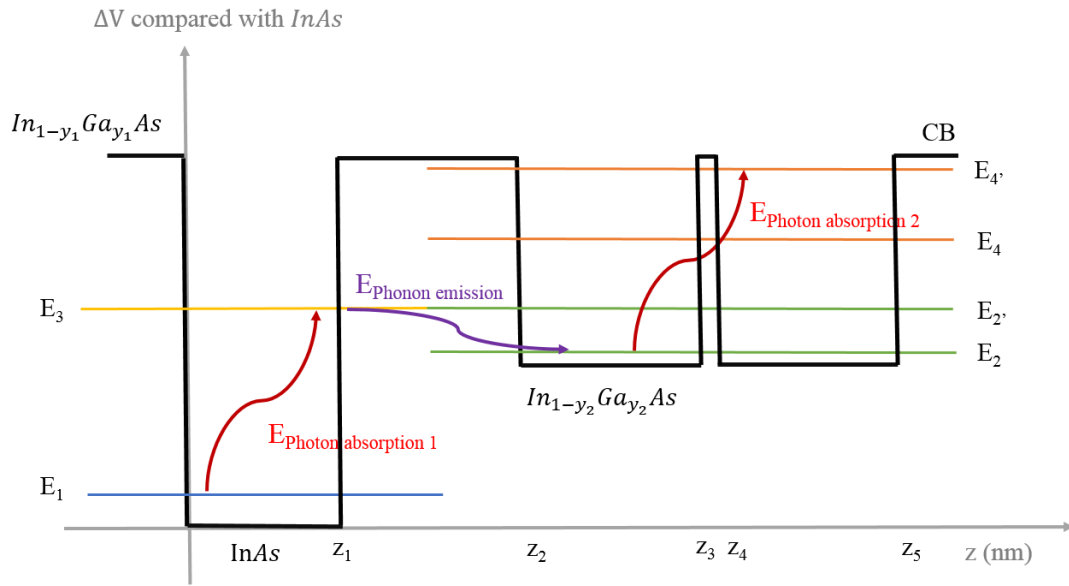**Figure 4. Simulation for Single-Double Quantum Well in In$_{1-y}$Ga$_y$As material.**

Figure 5. depicts the optimized structure for the design in InGaAs material based on many calculations performed by adjusting these parameters.
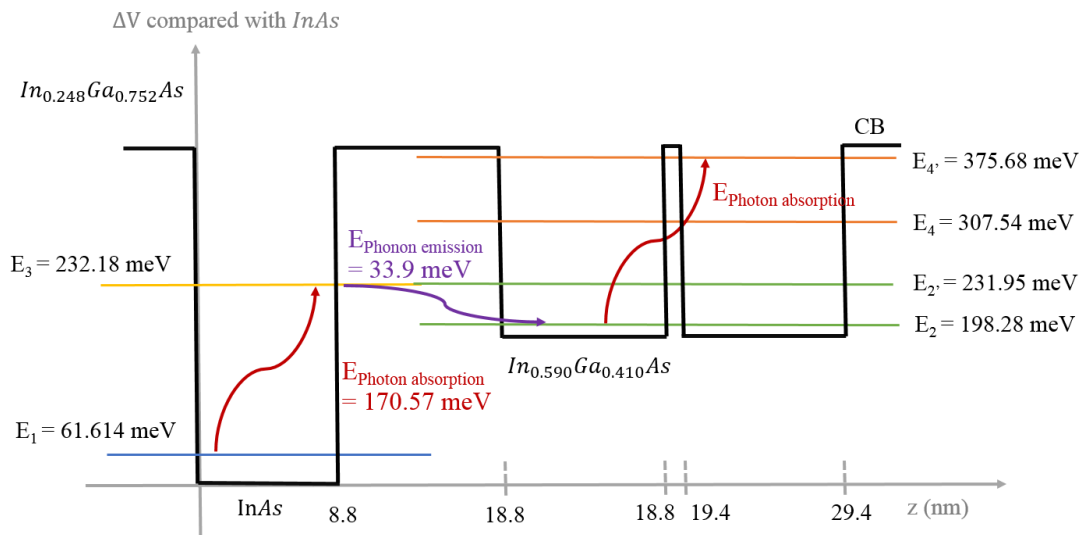
Figure 5. Optimized Signal-to-Noise enhanced photodetector in In$_{1-y}$Ga$_y$As material.

For the single well, In$_{0.248}$Ga$_{0.752}$As is used as the barrier, and InAs as the well. The potential of the single well then turns out to be 381.371 meV. For the double well, In$_{0.248}$Ga$_{0.752}$As is still the barrier, both outside the double well and between it, and now we use In$_{0.590}$Ga$_{0.410}$As as the well. A depth of 205.845 meV as the potential of the double well is obtained.

In this result, we have the width of single well as 8.8 nm, and the width of each well in double well as 10 nm. The barrier between the double well is 0.6 nm, and the barrier between single well and double well is 10 nm.

The energy states in single well then turn out to be E$_1$ = 61.614 meV, and E$_3$ = 232.18 meV. In the double well, energy states are E$_2$ = 198.28 meV, E$_{2'}$ = 231.95 meV, E$_4$ = 307.54 meV, and E$_{4'}$ = 375.68 meV as shown in Figure 5.

The whole process for this signal-to-noise photodetector with InGaAs material in this design works as following:

  i.   From E$_1$ state, an electron absorbs one photon energy which equals to 170.57meV, having wavelength of 7269.74 nm, and transitions to the E$_3$ state.

  ii.   The electron emits one phonon energy of 33.9 meV, with wavelength 36578.17 nm, and falls down to the state E$_2$.

  iii. Absorbing another phonon with 177.4 meV (wavelength = 6989.85 nm) which having similar energy as the first one, the electron transitions to E$_{4'}$, which is very close to the barrier level of In$_{0.248}$Ga$_{0.752}$As, and will be detected.

The photon absorption for the first photon and the second photon having a difference of 4% in energy. Even though, error less than 5% is acceptable in experiment, the light source being detected needs to have a wide band at least from 6989.85 nm to 7269.74 nm in this apparatus.

The parameters we need include: the discontinuity of conduction band energy for In$_{1-x}$Al$_x$As that having different concentration of x, the electron effective mass for the corresponding x value, and the conduction band energy level and electron effective mass of InP.

The total band gap energy discontinuity for In$_{1-x-y}$Al$_x$Ga$_y$As/AlAs is mentioned in the previous part as:

$$\Delta V = [2.093x + 0.629y + 0.577x^2 + 0.436y^2 + 1.013xy - 2.0x^2(1 - x - y)] \, eV$$

and the band alignment is 47% of the total discontinuity in valence band, which means:

$$\Delta V_{VB} = 0.47$$

$$\Delta V_{CB} = 0.53$$

The electron effective mass for $In_{1-x-y}Al_xGa_yAs/AlAs$ is:

$$m^* = (0.0427 + 0.0685x)m_0$$

where $m_0 = 9.10938215 \times 10^{-31}$.

Therefore, if $y = 0$ is assumed in all the parameters, we can get parameters for $In_{1-x}Al_xAs/AlAs$ as follows:

The total band discontinuity is:

$$\Delta V' = (2.093x - 1.423x^2 + 2x^3) \, eV$$

and since that $\Delta V_{VB} = 0.47$ and $\Delta V_{CB} = 0.53$, the conduction band discontinuity of $In_{1-y}Ga_yAs/AlAs$ is:

$$\Delta V'' = [(2.093x - 1.423x^2 + 2x^3) \times 0.53] \, eV$$

Also,

$$m^{*\prime} = (0.0427 + 0.0685x)m_0$$

where $m_0 = 9.10938215 \times 10^{-31}$.

The heterointerface in the InGaAs/InAlAs/InP family is described as follows:

For the conduction band energy level, $In_{0.52}Al_{0.48}As$ is 0.34 eV higher than InP.

The conduction band discontinuity of $In_{0.52}Al_{0.48}As$ to AlAs is 0.475921 eV.

The conduction band discontinuity of InAs to AlAs is 1.4151 eV.
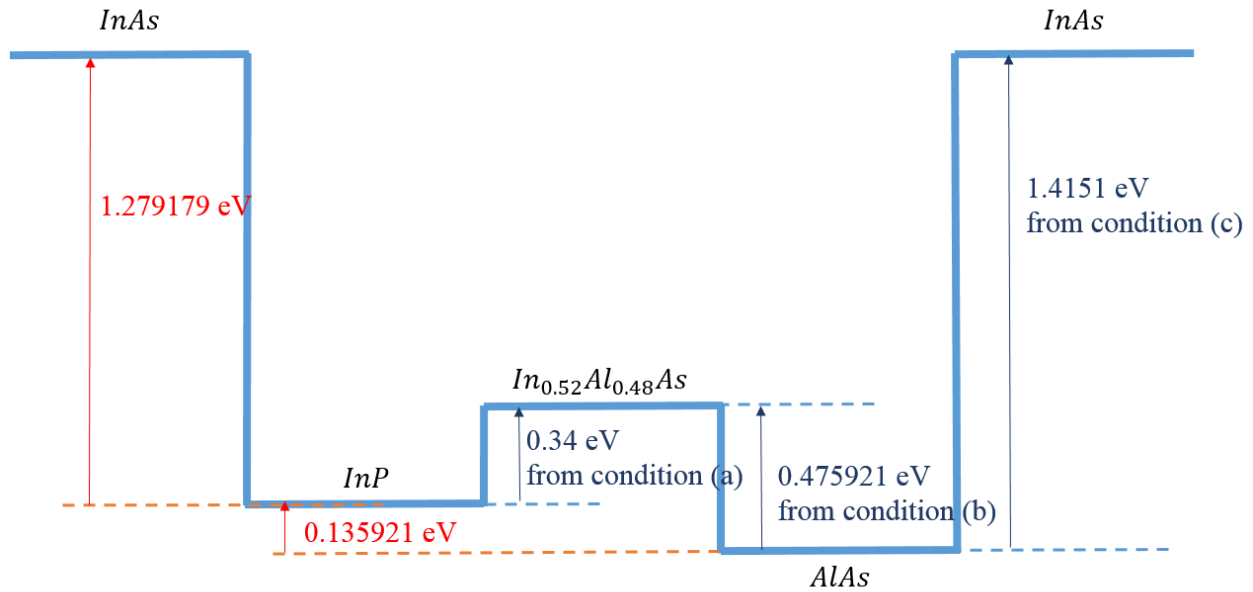
Figure 6 depicts the relevant energy conditions.

11

Figure 6..Conduction band energy level relationships of the In$_{0.52}$Al$_{0.48}$As/InAs/AlAs/ InP family.

As shown in Figure 6, we can calculate the conduction band discontinuity of InP to AlAs by substrate 0.475921 eV to 0.34 eV, so 0.135921 is obtained.

For the the conduction band discontinuity of InAs to InP: $1.4151\,\text{eV} - 0.135921\,\text{eV} = 1.279179\,\text{eV}$, which is the largest quantum well potential that we are able to design in InAlAs/InP design when using InP as the material of the single well.

For calculating the In$_{1-x}$Al$_x$As/InP conduction band discontinuity, the relationship of them is plotted as Figure 7.

12

$In_{1-x}Al_xAs$

$\Delta V''' = (\Delta V'' - 0.135921)\ eV$

$\Delta V'' = [(2.093x - 1.423x^2 + 2x^3) \times 0.53]\ eV$

InP

0.135921 eV

$AlAs$

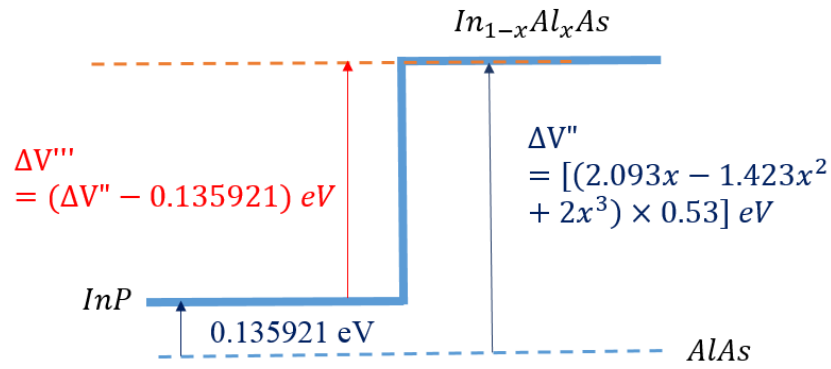**Figure7. Conduction band discontinuity of In$_{1-x}$Al$_x$As/InP.**

According to Figure 7,

$$\Delta V''' = (\Delta V'' - 0.135921)\ eV$$
$$= [(2.093x - 1.423x^2 + 2x^3) \times 0.53 - 0.135921]\ \text{eV}$$

Using the previously-defined parameters the single-double well design in In$_{1-x}$Al$_x$As/InP material is defined as illustrated in Fig. 8.
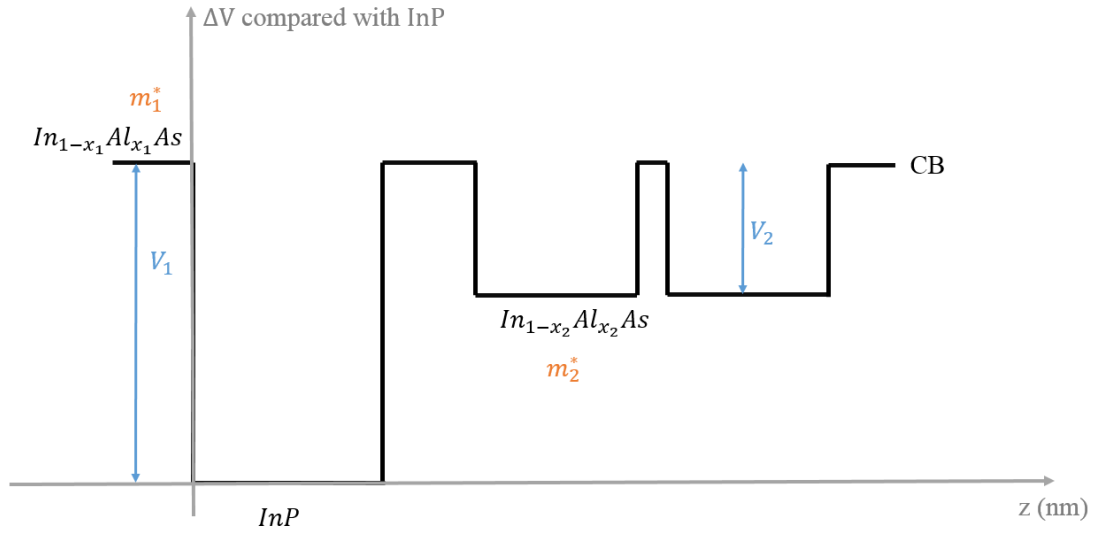
13

Figure 8. Single-Double Quantum Well Design in In$_{1-x}$Al$_x$As/InP material.

For the conduction band (CB) changes compared with InP conduction band is depicted in Figure 8 for the structure made consideration.

The value of V1 and V2 in Figure 14 are given in terms of:

$$V_1 = \left[(2.093x_1 - 1.423x_1^2 + 2x_1^3) \times 0.53 - 0.135921\right]$$

$$V_1 - V_2 = \left[(2.093x_2 - 1.423x_2^2 + 2x_2^3) \times 0.53 - 0.135921\right]$$

The corresponding electron effective masses are,

$$m_1^* = (0.0427 + 0.0685x_1)m_0$$

$$m_2^* = (0.0427 + 0.0685x_1)m_0$$

as well as $m_{InP}^* = 0.08m_0$.

The Schrödinger equations for solutions, as outlined previously, yield the following designs.

In the In$_{1-x}$Al$_x$As/InP design, the larger the x is, the higher the conduction band level will be.

14

ΔV compared with InP

$In_{1-x_1}Al_{x_1}As$ — CB

$E_{4'}$
E_4

$E_{Phonon\ emission}$

E_3
$E_{2'}$
E_2

$E_{Photon\ absorption\ 2}$

$E_{Photon\ absorption\ 1}$
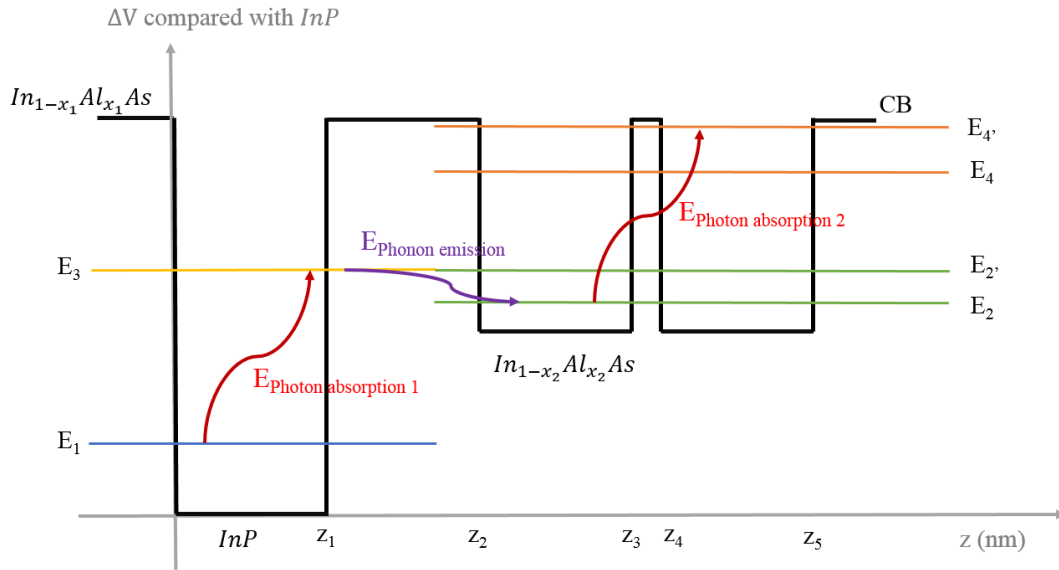
$In_{1-x_2}Al_{x_2}As$

E_1

InP z_1 z_2 z_3 z_4 z_5 z (nm)

Figure 9. Simulation for single-double quantum well in $In_{1-x}Al_xAs/InP$ material.

These results illustrate the feasibility of the phonon-assisted photodetector design in a variety of heterostructure systems.

The AlGaAs/GaAs triple quantum well photodetector (QWP) with a detection wavelength at 5 μm has been analyzed further as discussed in Tang et al. (2016) which was produced under this grant. It shows that the escape probability of phonon-assisted tunneling devices can be enhanced by over two times, if the condition of the electron-phonon resonance is accompanied by the anticrossing between first excited level in single QW and the first excited level in the adjacent double QW. The escape probability in the proposed triple QWP is optimized to be as high as 0.8, which is at least two times higher than reported in QCDs. In addition, the noise current in the proposed structure is studied to have a reduction of 2.9×10^{13} times that in a QWP at 77 K. Moreover, the effects of delta doping locations and densities on scattering time and absorption coefficient in AlGaAs/GaAs triple QWP have been studied theoretically. It shows that delta doping at the middle of the single well has advantages in obtaining longer intersubband relaxation time, larger escape probability and higher absorption coefficient. These results are especially valuable for designing double resonance optoelectronic device

A summary of results obtained during this effort this effort include: design of novel multi-quantum-well structures with greatly enhanced signal-to-noise in tailored structures that

employ phonon-assisted transition to enhance the effective ionization potential; spontaneous polarization induced electric field in zinc oxide nanowires and nanostars; and enhanced optical properties due to indium incorporation in zinc oxide nanowires.

Summary: Specific results were obtained on the following topics: phononic properties for enhanced signal-to-noise photodetector; spontaneous polarization induced electric field in nanostructures; AlGaAs/GaAs triple well photodetector design based on phonon-assisted transitions operating at a 5-micron wavelength with greatly reduced noise – noise reduced several orders of magnitude at room temperature; and enhanced optical properties due to indium incorporation in zinc oxide nanowires.

REFERENCES

Kisin, Mikhail V., Vera B. Gorfinkel, Michael A. Stroscio, Gregory Belenky, and Serge Luryi, Influence of Complex Phonon Spectra on Intersubband Optical Gain, Journal of Applied Physics, 82, 2031 (1997).

Lan, Yi, Nanzhu Zhang, J. (Lucy) Shi, M. Dutta, M. A. Stroscio, "Enhanced signal-to-noise in photodetectors due to interface phonon-assisted transitions, 2014 International Workshop on Computational Electronics (IWCE), Paris, INSPEC Accession Number: 14485107, August 2014: IEEE: DOI: 10.1109/IWCE.2014.6865857

Menon, V. M., L. R. Ram-Mohan, W. D. Goodhue, A. J. Gatesman, A. S. Karakashian, Role of Interface Phonons in Quantum Cascade Terahertz Emitters, Physica B, 316-317, 212-215 (2002).

Tang, Chenjie, Lan, Yi, Dutta, Mitra, Stroscio, Michael A., and Shi, Junxia, GaAs/GaAs Triple Quantum Well Photodetector at 5μm Wavelength, IEEE Journal of Quantum Electronics, 52(11), 1-8 440108 (2016).

Spagnolo V., , G. Scamarcio, M. Troccoli, F, Capasso, C. Gmachl, A. M. Sergent, A. L. Hutcheson, D. L. Sivco, and A. Y. Cho, Nonequilibrium Optical Phonon Gen. by Steady State Electron Transport in Quantum-Cascade Lasers, APL, 80, 4303-4305 (2002)

Stroscio, Michael A., Interface-Phonon--Assisted Transitions in Quantum Well Lasers, Journal of Applied Physics, 80, 6864 (1996).

Stroscio, Michael A., Mihail Kisin, Gregory Belenke, and Serge Luryi, Phonon enhanced inverse population in asymmetric double quantum wells, Appl. Phys. Letts., 75, 3258-3260 (1999).

Stroscio, M., and M. Dutta, Phonons in Nanostructures (Cambridge University Press. 2001).

Williams, B. S., B. Xu, Q. Hu, Narrow-linewidth Terahertz Emission from Three-level Systems, APL, 75, 2927 (1999)

(5) List of Publications and Technical Reports

<u>PAPERS PUBLISHED</u>

Archival Publications (published) during reporting period:

S. Farid, M. Choi, D. Datta, M. A. Stroscio and M. Dutta, Spontaneous polarization induced electric field in zinc oxide nanowires and nanostars, Journal of Applied Physics, 119, 163108 (2016).

S. Farid, S. Mukherjee, K. Sarkar, M. Mazouchi, M. A. Stroscio and M. Dutta, Enhanced optical properties due to indium incorporation in zinc oxide nanowires, Appl. Phys. Lett. 108, 021106 (2016).

Yi Lan, Chenjie Tang, Junxia (Lucy) Shi, Mitra Dutta, Michael Stroscio, Phononic Properties for Enhanced Signal-to-Noise Photodetector, Proceedings of the 18th International Workshop on Computational Electronics, DOI: 10.1109/IWCE.2015.7301969 ISBN978-0-692-51523-5/15 Copyright 2015 IEEE.

Chenjie Tang, Yi Lan, Mitra Dutta, Michael A. Stroscio, and Junxia Shi, GaAs/GaAs Triple Quantum Well Photodetector at 5μm Wavelength, IEEE Journal of Quantum Electronics, 52(11), 1-8 440108 (2016).

PRESENTATION - PEER REVIEWED

Yi Lan, Chenjie Tang, Junxia (Lucy) Shi, Mitra Dutta, Michael Stroscio, Phononic Properties for Enhanced Signal-to-Noise Photodetector, Proceedings of the 18th International Workshop on Computational Electronics, Purdue University, September 2016.

(6) List of All Participating Scientific Personnel

Michael A. Stroscio, PI
Mitra Dutta, Co-PI
Lucy Shi, Co-PI
Chenjie Tang
Yi Lan
Ketaki Sarkar
Ahmed Mohammad

(7) Honors and Awards

The PI was:

Appointed as a University Distinguished Professor (2015); typically 3 or 4 UIC professors are selected each year.

Reappointed as the Richard and Loan Hill Professor (2017)

Award for Excellence in Teaching (2017) - typically 3 or 4 UIC professors are selected each year. This is UIC's highest teaching award.

Elected to the College of Fellows, American Institute of Medical and Biomedical Engineers

(8) Report of Inventions: None

AFOSR Deliverables Submission Survey

Response ID:8020 Data

1.

Report Type

Final Report

Primary Contact Email
Contact email if there is a problem with the report.

stroscio@uic.edu

Primary Contact Phone Number
Contact phone number if there is a problem with the report

8479624955

Organization / Institution name

Univ. of IL at Chicago

Grant/Contract Title
The full title of the funded effort.

Quantum Engineering of States in Heterostructure-based Detectors for Enhanced Performance

Grant/Contract Number
AFOSR assigned control number. It must begin with "FA9550" or "F49620" or "FA2386".

FA9550-15-1-0493

Principal Investigator Name
The full name of the principal investigator on the grant or contract.

Michael A. Stroscio

Program Officer
The AFOSR Program Officer currently assigned to the award

Dr. Kenneth C. Goretta

Reporting Period Start Date

09/30/2015

Reporting Period End Date

03/29/2017

Abstract

This research effort has the goals of exploiting and integrating forefront developments in nanoscience and nanoelectronics to conceive, design, fabricate, and test flexible sensors with greatly enhanced performance. To accomplish these goals, this effort focused on the design of novel heterostructure-based sensors that integrate multiple-quantum-well elements to yield enhanced performance based on quantum engineering of both electronic and phononic states. Specifically, in this work the unwanted thermally excited carrier contribution in these heterostructure-based photodetectors has been reduced by using phonon-assisted transitions to design structures having deeper initial quantum states. This novel design has been modeled and characterized experimentally for a prototypical heterostructure. In addition, this effort addressed the optimization of these photodetectors through tailoring carrier interactions in these reduced dimensional structures. This research program addressed systematic theoretical and experimental investigations of nanostructure-based electronic and optoelectronic

structures with the goal of facilitating major improvements in the performance levels of nanodevices beyond the current state-of-the-art. In particular, this program focuses on research thrusts with objectives including: model, design, fabricate, and experimentally characterize nano-device structures for enhanced charge transport & collection; model, design, fabricate, and experimentally characterize such nanodevices to optimize device structures with quantum-engineering and phonon-assisted transitions in nanostructures. Quantum engineering of nano-structures is emphasized. Related quantum-based structures – including those with spontaneous polarizations are included.

Distribution Statement
This is block 12 on the SF298 form.

Distribution A - Approved for Public Release

Explanation for Distribution Statement
If this is not approved for public release, please provide a short explanation. E.g., contains proprietary information.

SF298 Form
Please attach your SF298 form. A blank SF298 can be found here. Please do not password protect or secure the PDF The maximum file size for an SF298 is 50MB.

AFOSR_sf_298_May_2017_BEST.pdf

Upload the Report Document. File must be a PDF. Please do not password protect or secure the PDF . The maximum file size for the Report Document is 50MB.

AFOSR_Report_May_2017.pdf

Upload a Report Document, if any. The maximum file size for the Report Document is 50MB.

Archival Publications (published) during reporting period:

PAPERS PUBLISHED

Archival Publications (published):

S. Farid, M. Choi, D. Datta, M. A. Stroscio and M. Dutta, Spontaneous polarization induced electric field in zinc oxide nanowires and nanostars, Journal of Applied Physics, 119, 163108 (2016).

S. Farid, S. Mukherjee, K. Sarkar, M. Mazouchi, M. A. Stroscio and M. Dutta, Enhanced optical properties due to indium incorporation in zinc oxide nanowires, Appl. Phys. Lett. 108, 021106 (2016).

Yi Lan, Chenjie Tang, Junxia (Lucy) Shi, Mitra Dutta, Michael Stroscio, Phononic Properties for Enhanced Signal-to-Noise Photodetector, Proceedings of the 18th International Workshop on
Computational Electronics, DOI: 10.1109/IWCE.2015.7301969 ISBN978-0-692-51523-5/15 Copyright 2015 IEEE.

Chenjie Tang, Yi Lan, Mitra Dutta, Michael A. Stroscio, and Junxia Shi, GaAs/GaAs Triple Quantum Well Photodetector at 5μm Wavelength, IEEE Journal of Quantum Electronics, 52(11), 1-8 440108 (2016).

PRESENTATION - PEER REVIEWED

Yi Lan, Chenjie Tang, Junxia (Lucy) Shi, Mitra Dutta, Michael Stroscio, Phononic Properties for Enhanced Signal-to-Noise Photodetector, Proceedings of the 18th International Workshop on Computational Electronics, Purdue University, September 2016.

New discoveries, inventions, or patent disclosures:

Do you have any discoveries, inventions, or patent disclosures to report for this period?

No

> **Please describe and include any notable dates**

> **Do you plan to pursue a claim for personal or organizational intellectual property?**

Changes in research objectives (if any):

N/A

Change in AFOSR Program Officer, if any:

N/A

Extensions granted or milestones slipped, if any:

N/A

AFOSR LRIR Number

LRIR Title

Reporting Period

Laboratory Task Manager

Program Officer

Research Objectives

Technical Summary

Funding Summary by Cost Category (by FY, $K)

	Starting FY	FY+1	FY+2
Salary			
Equipment/Facilities			
Supplies			
Total			

Report Document

Report Document - Text Analysis

Report Document - Text Analysis

Appendix Documents

2. Thank You

E-mail user

May 26, 2017 11:01:56 Success: Email Sent to: stroscio@uic.edu